Temperature" (to be published).
[4]B. I. Halperin and P. C. Hohenberg, Phys. Rev. 188, 898 (1969).
[5]K. H. Michel and F. Schwabl, Z. Phys. 238, 264 (1970).
[6]E. Prohofsky and J. Krumhansl, Phys. Rev. 133, A1403 (1964). The analog of second sound for magnetic systems has been put forward by Y. U. Gulayev, Zh. Eksp. Teor. Fiz., Pis'ma Red. 2, 3 (1965) [JETP Lett. 2, 1 (1965)]; R. N Ghurzi, Fiz. Tverd. Tela 7, 3515 (1966) [Sov. Phys. Solid State 7, 2838 (1966)]; G. F. Reiter, Phys. Rev. 175, 631 (1968); I. N. Oleinik, Zh. Eksp. Teor. Fiz. 58, 1119 (1970) [Sov. Phys. JETP 31, 600 (1970)]; K. H. Michel and F. Schwabl, Solid State Commun. 7, 1781 (1969), and Phys. Kondens. Mater. 11, 144 (1970); F. Schwabl and K. H. Michel, Phys. Rev. B 2, 189 (1970); Michel and Schwabl, Ref. 5.
[7]K. C. Turberfield, A. Akazaki, and R. W. Stevenson, Proc. Phys. Soc., London 85, 743 (1965).
[8]R. J. Joenk, Phys. Rev. 128, 1634 (1962). See also F. Keffer, in *Handbuch der Physik*, edited by H. P. J. Wijn (Springer, Berlin, 1966), Vol. XVIII, Pt. 2, p. 110.
[9]Michel and Schwabl, Ref. 6.
[10]Schwabl and Michel, Ref. 6.
[11]J. Skalyo, Jr., private communication.

Facet-Related Site Selectivity for Rare-Earth Ions in Yttrium Aluminum Garnet

R. Wolfe, M. D. Sturge, F. R. Merritt, and L. G. Van Uitert
Bell Telephone Laboratories, Murray Hill, New Jersey 07974
(Received 10 May 1971)

We have measured the spin-resonance spectra of crystals cut from beneath {110} and {112} facets of flux-grown yttrium aluminum garnet doped with Nd^{3+} and Yb^{3+}. Sites which are crystallographically equivalent, but differ in their orientation relative to the facet normal, are found to be unequally populated. Such site preference can account in principle for the recently reported noncubic magnetocrystalline anisotropy of mixed rare-earth iron garnets.

The garnet structure is cubic, but recently it has been found that certain flux-grown mixed rare-earth iron garnets have noncubic magnetic properties which are associated with {110}- and {112}-type growth facets.[1-3] It has been proposed[4,5] that this anisotropy is due to a small preferential occupation of the rare-earth sites; i.e., the different rare-earth ions are not randomly distributed over crystallographically equivalent sites, but prefer sites oriented in a particular way relative to the facet normal. Such a nonrandom distribution of Gd^{3+} ions in flux-grown Al_2O_3 was found many years ago[6]; however, the connection with facet growth could not be made at that time. Facet-related site selectivity has been reported for natural amethyst,[7] which is α-quartz in which Fe^{3+} substitutes for some Si^{4+} ions.

In this Letter we report spin resonance measurements that demonstrate facet-related site selectivity for Nd^{3+} and Yb^{3+} ions in flux-grown yttrium aluminum garnet (YAlG). In a magnetic garnet, such selectivity would be amply large enough to account for the noncubic anisotropy observed. Sites that are equivalent with respect to the facet normal are equally populated, while those that are inequivalent are not, in general. The sense of the preference changes on going from Nd^{3+}, which is 12% larger in ionic radius than the Y^{3+} ion it replaces, to Yb^{3+}, which is 4% smaller. This suggests that one can use ionic radius differences to predict site preference.

The garnets were grown from a PbO-PbF_2-B_2O_3 flux by cooling at $\frac{1}{2}°$/h from 1300 to 950°C.[8] The crucible was then drained of flux while still within the furnace and the crystals were slowly cooled to prevent thermal shock. Specimens were cut from material just beneath the surface near the center of two adjacent facets, one of the {110} and one of the {112} type, and oriented by x rays with an accuracy of $\pm\frac{1}{4}°$.

There are six magnetically inequivalent types of dodecahedral (Y^{3+}) sites in garnet.[9] These sites have D_{2h} symmetry with the principal axes given in Table I. The sites fall into groups which are equivalent with respect to [110] and [112] (the normals to the two principal types of facets in garnet) as shown in columns 5 and 6 of Table I.

We measured the relative intensity of the spin-resonance transitions from each site at 24 GHz and 4.2°K. While the $S=\frac{1}{2}$ orthorhombic spin Hamiltonian given in the literature[10] fits the positions of the resonances of Nd^{3+} and Yb^{3+} accurate-

Table I. Dodecahedral sites in garnet.

Site[a]	Axes x	y	z	Site equivalence (110) facet	(112) facet
X_1	$01\bar{1}$	011	100	X	X_1
X_2	011	$01\bar{1}$	$\bar{1}00$	X	X_2
Y_1	$\bar{1}01$	101	010	X	X_1
Y_2	101	$\bar{1}01$	$0\bar{1}0$	X	X_2
Z_1	$1\bar{1}0$	110	001	Z_1	Z_1
Z_2	110	$1\bar{1}0$	$00\bar{1}$	Z_2	Z_2

[a]Rosencwaig's notation (Ref. 4). His "barred" sites ($\bar{X}_1$, etc.), are related to the above six by inversion, and are magnetically equivalent to them.

ly, and the intensities for Yb^{3+}, it fails to account for a pronounced dependence of the Nd^{3+} intensities on the direction of the dc magnetic field H_{dc}. (For a fixed orientation of the microwave field H_{rf}, there should be no such dependence.) This is probably because H_{dc} mixes low-lying excited states of the $J=\frac{9}{2}$ manifold into the ground state. Since one cannot calculate this effect accurately, we designed our procedure to determine site populations independently of transition probabilities. H_{dc} was rotated successively in planes close to (110), (101), and $(1\bar{1}0)$ [the growth plane being defined as (110) or (112)]. H_{rf} was perpendicular to the plane of rotation. This plane was tilted about 2° from the symmetry plane in order to separate the resonance lines as associated with each site. When H_{dc} crosses a mirror plane, the lines from each site change places, as illustrated in Fig. 1. This shows some resonances obtained from a sample of YAlG:Nd^{3+} cut from a (112) facet. In (a) and (c) H_{dc} is rotated in a plane near (110); (b) shows the angular dependence of the resonance fields. Sites Y_2, X_1, Y_1, and X_2 in (a) are respectively magnetically equivalent to X_2, Y_1, X_1, and Y_2 in (c), where H_{dc} is on the opposite side of the intersection with $(1\bar{1}0)$ (a mirror plane). Since the transition probability is the same for magnetically equivalent transitions, the population ratios $[X_1]/[Y_1]$ and $[X_2]/[Y_2]$ are equal to the ratios of the corresponding integrated areas. We see that in (a) and (c) the integrated areas of corresponding transitions, and hence the site populations, are equal. In (d) and (e), on the other hand, the plane of rotation is near (101), and we compare sites Z_2, X_1, Z_1, and X_2 in (d) with X_2, Z_1, X_1, and Z_2 in (e). Thus we obtain the population ratios $[Z_1]/[X_1]$ and $[Z_2]/[X_2]$; the difference in population is obvious from the spectra. The third plane, near $(1\bar{1}0)$ (not shown), gives us the ratios $[X_1]/[Y_2]$ and $[X_2]/[Y_1]$.

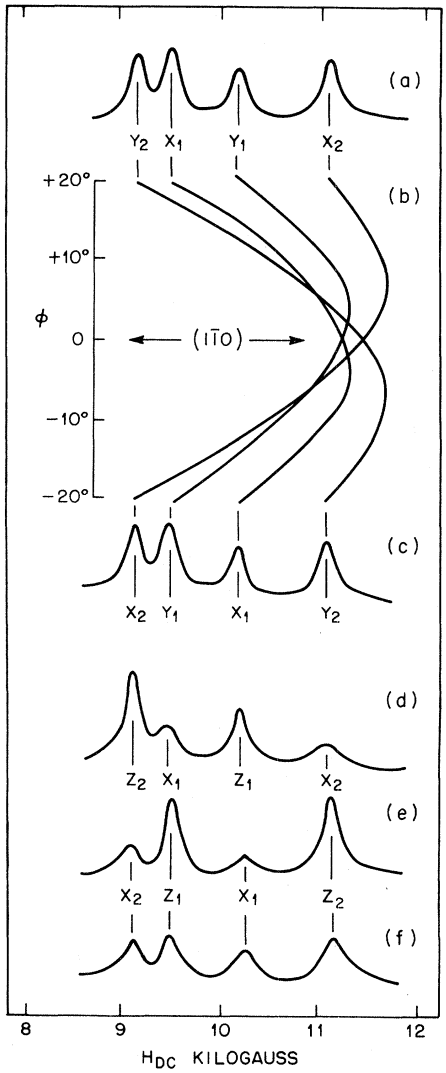

FIG. 1. Part of the spin-resonance spectrum of Nd^{3+} in YAlG. The idealized spectra are for a sample cut from a (112) facet. (a) H_{dc} is in a plane tilted 2° from (110), clockwise about $[\bar{1}10]$, with $\varphi=+20°$ {φ is measured in the plane of rotation from the intersection with $(1\bar{1}0)$ near [001], towards $[1\bar{1}0]$}. (b) Dependence of the resonance fields on φ as H_{dc} is rotated in a plane 2° from a (110)-type plane. (c) Same as (a), with $\varphi=-20°$. Comparison with (a) shows that the populations of the X and Y sites are equal within experimental error. (d) H_{dc} is in a plane tilted 2° from (101), clockwise about $[10\bar{1}]$, with $\varphi=+20°$ {measured from the intersection with $(10\bar{1})$ near [010], towards $[10\bar{1}]$}. The angular dependence of the resonance fields is the same as in (b). (e) Same as (d), but with $\varphi=-20°$. Comparison with (d) shows that Z sites are much more heavily populated than X sites. (f) Same as (e), after annealing. The Z and X site populations have almost equalized.

Quantitative results, which were obtained by

Table II. Relative populations of impurity ions in dodecahedral sites of YAlG.

Impurity (approx. at.%)	Facet	Rel. pop. ($[X] \approx [Y] \equiv 1$) $[Z_1]$	$[Z_2]$	Accuracy (%)
3% Nd	(110)	0.65	0.60	10
3% Nd	(112)	2.3	3.5	10
1% Yb	(110)	1.18	1.12	5
1% Yb	(112)	0.93	0.91	7
3% Nd (annealed)	(112)	1.15	1.3	15

averaging over many spectra like those shown, are summarized in Table II. The populations of sites X_1, X_2, Y_1, Y_2 never differ from each other by more than the experimental error, even for samples cut from {112} facets, for which symmetry permits a difference (see Table I). The average population of these sites is taken as unity, and Table II gives the populations of sites Z_1 and Z_2 relative to this average. Under a {110} facet a Z site is found to have only a 60 to 65% chance (relative to an X or Y site) of being occupied by a Nd^{3+} ion. Under a {112} facet, on the other hand, a Z_1 site is 2.3 times, and a Z_2 site 3.5 times, as likely as an X or Y site to be occupied. The differences for Yb^{3+} are smaller, but still significant. Note that the assignment of particular resonances to sites Z_1 and Z_2 (rather than the other way round) is arbitrary. We follow the convention of Ref. 10 in assigning the g factors, but since there is no adequate theory of the g factors this convention has no microscopic significance. In particular, the assignment can change on going from Nd^{3+} to Yb^{3+}.

We annealed one of our samples for 20 h at 1250°C in an oxygen atmosphere. This treatment is known[2] to eliminate noncubic magnetic anisotropy in the rare-earth iron garnets. The data of Table II and the figure [spectrum (f)] show that the site preference in YAlG is greatly reduced, although not completely eliminated, by this treatment. This shows that the rare-earth ions diffuse at this temperature. The effect of rare-earth concentration was checked by studying a sample doped with approximately 0.1% Nd cut from a (110) facet. Site preferences are a little more pronounced in this sample, but essentially the results are the same as for the corresponding 3% crystal.

We see from Table II that Nd^{3+} (larger than Y^{3+}) prefers sites where the local z axis is as close as possible to the facet normal, while Yb^{3+} (smaller than Y^{3+}) shows the reverse perference. While this shows that ionic radius is likely to be a useful phenomenological guide to site preference, we would not be justified in deducing that such preference is necessarily a stereochemical phenomenon. Many chemical properties, for instance electronegativity, are monotonic functions of ionic radius within the III*b* group (which includes the rare earths) and different chemical mechanisms cannot be distinguished by our measurements.

Our results cannot be used directly to predict quantitatively the noncubic magnetocrystalline anisotropy of mixed rare-earth iron garnets. We deliberately chose to study dilute mixtures of ions differing greatly in ionic radius, in order to maximize the site selectivity. The magnetic garnets which show uniaxial anisotropy are usually concentrated mixtures of rare-earth ions. The site selectivity in such materials need only be of order 1% to account in principle for the noncubic anisotropy observed.

Equal population of the Z_1 and Z_2 sites would imply uniaxial anisotropy[4,5]; this is indeed observed (to a good approximation) under the {110} facets of some magnetic garnets.[3] In others, however, the anisotropy is orthorhombic,[2] as it almost always is under {112} facets.[1] Such orthorhombic anisotropy implies that the Z_1-Z_2 population difference is as important as the Z-(X, Y) difference. While our qualitative result, that pronounced facet-related site selectivity occurs in garnets, is certainly applicable to the magnetic problem, quantitative predictions will have to await measurements on more closely related materials.

We are grateful to F. C. Frank, S. Geschwind, J. E. Geusic, E. M. Gyorgy, and R. D. Pierce for helpful discussions; to A. J. Kurtzig for annealing a crystal; and to Miss S. M. Vincent for x-ray fluorescence analysis.

[1]A. H. Bobeck, E. G. Spencer, L. G. Van Uitert, S. C. Abrahams, R. L. Barns, W. H. Grodkiewicz, R. C. Sherwood, P. H. Schmidt, D. H. Smith, and E. M. Walters, Appl. Phys. Lett. 17, 131 (1970).

[2]R. C. Le Craw, R. Wolfe, A. H. Bobeck, R. D. Pierce, and L. G. Van Uitert, J. Appl. Phys. 42, 1641 (1971).

[3]A. Rosencwaig, W. J. Tabor, F. B. Hagedorn, and L. G. Van Uitert, Phys. Rev. Lett. 26, 775 (1971).

[4]A. Rosencwaig and W. J. Tabor, J. Appl. Phys. 42, 1643 (1971); A. Rosencwaig, W. J. Tabor, and R. D. Pierce, Phys. Rev. Lett. 26, 779 (1971).

[5]H. Callen, Appl. Phys. Lett. 18, 311 (1971).

[6]S. Geschwind and J. P. Remeika, Phys. Rev. 122, 757 (1961).

[7]T. I. Barry, P. McNamara, and W. J. Moore, J. Chem. Phys. 42, 2599 (1965).

[8]L. G. Van Uitert, W. H. Grodkiewicz, and E. F. Dearborn, J. Amer. Ceram. Soc. 48, 105 (1965).

[9]See, for instance, J. F. Dillon and L. R. Walker, Phys. Rev. 124, 1401 (1961).

[10]W. P. Wolf, M. Ball, M. T. Hutchings, M. J. M. Leask, and A. F. G. Wyatt, J. Phys. Soc. Jap., Suppl. 17, B-I, 443.

Variation of Characteristic Energy Losses in the Curie-Temperature Region of Ni (111)

B. Heimann and J. Hölzl

Institut für Experimentalphysik der Technische Universität Clausthal, Clausthal-Zellerfeld, Germany

(Received 31 March 1971)

We have studied the temperature dependence of characteristic energy losses of slow electrons scattered from a Ni (111) surface. The volume loss energy shows an anomalous variation in the region of Curie temperature superimposed on a linear decrease from $T = 100$ to 700°C.

In an earlier publication[1] we studied the temperature dependence of secondary electron emission of polycrystalline Ni in the region of the Curie temperature T_C. In this paper we present the results of an experimental investigation of the spectrum of characteristic energy losses (CEL). In particular, CEL measurements will be discussed both as a function of temperature T ($100 \leq T \leq 700$°C) and primary energy E_p ($150 \leq E_p \leq 600$ eV).

In earlier studies[2,3] of the CEL spectra of electrons scattered from Ni, no variation in the energy of the CEL as a function of temperature was observed. Jordan,[3] in particular, reports CEL at 8.5 and 19.0 eV using a Ni (100) surface, which he interprets in accordance with Robins and Swan[4] as the surface and volume plasma energy losses, respectively. An additional loss at 28.0 eV is tentatively ascribed by Jordan[3] to both the combined bulk and surface plasmon exitation and an interband transition.

In the present experiment a Ni (111) surface is studied in a retarding-field analyzer with an energy resolution of $\Delta E/E = 0.5\%$. Special attention was given to the cleanliness of the crystal surface. The starting material was a 99.999% pure single crystal of Ni. Cleaning was done by oxidation, reduction, and thermal treatment.[5] Auger measurements and CEL, both being very sensitive to small surface contaminations, were used to demonstrate the cleanliness of the surface. All measurements were done in an ultrahigh vacuum system at pressures $p < 1 \times 10^{-10}$ Torr.

A typical energy spectrum, measured at $T = 200$°C and with a primary energy $E_p = 150$ eV is shown in Fig. 1. Some of the CEL detected by our experiments are clearly visible in this spectrum. Using various primary energies and the second derivative of the retarding-field curves, the following characteristic energy losses were observed at $T = 200$°C: $E_1 = 1.9$ eV; $E_2 = 3.4$ eV; $E_3 = 8.1$ eV; $E_4 = 11.0$ eV; $E_5 = 16.2$ eV; $E_6 = 19.1$ eV; $E_7 = 26.7$ eV; $E_8 = 33.2$ eV; $E_9 = 42.5$ eV; and $E_{10} = 67.0$ eV. The maximum experimental error of all loss energies measured was ±0.2 eV.

Following Jordan's interpretation, which is supported by his own optical measurements, it appears reasonable to attribute the energy losses $E_3 = 8.1$ eV and $E_6 = 19.1$ eV to the surface and volume plasma losses, respectively. With regard to the positions and intensities we attribute the loss energies $E_5 = 16.2$ eV and $E_9 = 42.5$ eV to the twofold surface and volume plasma losses, respectively. In this note we do not attempt to give an interpretation of the loss energies E_1, E_2, E_4, E_7, E_8, and E_{10}. The positions of these losses showed no variation with temperature.

The temperature dependence of the loss energies E_3 and E_6 as obtained with $E_p = 150$ eV is presented in Fig. 2. The following characteris-